4. Materials and methods are available as supporting material on *Science* Online.
5. A. J. Enright, S. Van Dongen, C. A. Ouzounis, *Nucleic Acids Res.* **30**, 1575 (2002).
6. T. Y. Sam-Yellowe *et al.*, *Genome Res.* **14**, 1052 (2004).
7. H. A. del Portillo *et al.*, *Nature* **410**, 839 (2001).
8. K. Fischer *et al.*, *Mol. Microbiol.* **48**, 1209 (2003).
9. C. S. Janssen, M. P. Barrett, C. M. Turner, R. S. Phillips, *Proc. R. Soc. London Ser. B* **269**, 431 (2002).
10. L. D. Stein *et al.*, *PLoS Biol.* **1**, E45 (2003).
11. T. Endo, K. Ikeo, T. Gojobori, *Mol. Biol. Evol.* **13**, 685 (1996).
12. R. H. Waterston *et al.*, *Nature* **420**, 520 (2002).
13. Y. S. Han, J. Thompson, F. C. Kafatos, C. Barillas-Mury, *EMBO J.* **19**, 6030 (2000).
14. M. P. Washburn, D. Wolters, J. R. Yates III, *Nature Biotechnol.* **19**, 242 (2001).
15. K. Vickerman, *Nature* **208**, 762 (1965).
16. J. Krungkrai, P. Prapunwattana, S. R. Krungkrai, *Parasite* **7**, 19 (2000).
17. K. Kaiser *et al.*, *Mol. Biochem. Parasitol.* **133**, 15 (2004).
18. J. B. Plotkin, J. Dushoff, H. B. Fraser, *Nature* **428**, 942 (2004).
19. M. M. Mota, J. C. Hafalla, A. Rodriguez, *Nature Med.* **8**, 1318 (2002).
20. K. G. Le Roch *et al.*, *Science* **301**, 1503 (2003).
21. L. Florens *et al.*, *Nature* **419**, 520 (2002).
22. Z. Bozdech *et al.*, *PLoS Biol.* **1**, E5 (2003).
23. A. P. Waters, *Science* **301**, 1487 (2003).
24. M. G. Paton *et al.*, *Mol. Biochem. Parasitol.* **59**, 263 (1993).
25. L. Cui, Q. Fan, J. Li, *Nucleic Acids Res.* **30**, 4607 (2002).
26. R. E. Hayward *et al.*, *Mol. Microbiol.* **35**, 6 (2000).
27. T. L. Bailey, M. Gribskov, *J. Comput. Biol.* **5**, 211 (1998).
28. R. M. Coulson, N. Hall, C. A. Ouzounis, *Genome Res.* **14**, 1548 (2004).
29. G. E. Crooks, G. Hon, J. M. Chandonia, S. E. Brenner, *Genome Res.* **14**, 1188 (2004).
30. We thank J. Dame (University of Florida) for the gift of the *P. berghei* GSS library, J. Langhorne (National Institute of Medical Research) for providing *P. c. chabaudi* DNA, R. G. Sadygov (The Scripps Research Institute) for expert computer programming, G. Butcher (Imperial College London) and M. Gardner (TIGR) for helpful advice with this manuscript, and M. Aslett and T. Kulikova for assisting with the database submission. Supported by the Wellcome Trust, the European Union, the Office of Naval Research, the U.S. Army Medical Research and Materiel Command, and the NIH. J.D.R. and J.M. are funded by the Wellcome Trust, M.K. by EU grant nos. RTN1-1999-00008 and QLK2-CT-1999-00753 and grant no. 050-10-053 from the Nederlands organisatie voor Wetenschappelijk Onderzoek, and H.E.T. by the EU MALTRANS consortium. The sequences have been submitted to EMBL under the accession prefixes CAAI for *P. berghei* and CAAJ for *P. chabaudi*. All data sets are available through the *Plasmodium* genome sequence data repository, PlasmoDB, at www.plasmodb.org and genome annotation at www.genedb.org.

Supporting Online Material
www.sciencemag.org/cgi/content/full/307/5706/82/DC1
Materials and Methods
Figs. S1 to S19
Tables S1 to S11
References and Notes

6 August 2004; accepted 2 November 2004
10.1126/science.1103717

REPORTS

Gigantic Photoresponse in ¼-Filled-Band Organic Salt $(EDO\text{-}TTF)_2PF_6$

Matthieu Chollet,[1] Laurent Guerin,[1,2] Naoki Uchida,[1] Souichi Fukaya,[1] Hiroaki Shimoda,[1] Tadahiko Ishikawa,[1] Kazunari Matsuda,[3] Takumi Hasegawa,[4] Akira Ota,[5] Hideki Yamochi,[6,8] Gunzi Saito,[5] Ryoko Tazaki,[7,8,9] Shin-ichi Adachi,[7,8] Shin-ya Koshihara[1,7,8]*

We report that the organic salt $(EDO\text{-}TTF)_2PF_6$ with ¾-filled-band (¼-filled in terms of holes), which forms an organic metal with strong electron and lattice correlation, shows a highly sensitive response to photoexcitation. An ultrafast, photoinduced phase transition from the insulator phase to the metal phase can be induced with very weak excitation intensity at near room temperature. This response makes the material attractive for applications in switching devices with room-temperature operation. The observed photoinduced spectroscopic change shows that this photoinduced phase transition process is caused by the cooperative melting of charge ordering assisted by coherent phonon generation.

Organic charge transfer (CT) A_2B salts composed of a cation (or anion) "A" and a counter ionic "B" in the ratio of 2:1 can display a variety of electronic and magnetic properties, such as superconductivity (*1*, *2*), metal-insulator (M-I) transition (*1*–*3*), magnetic frustration (*4*), ferroelectricity (*5*), and even magneto-dielectric coupled behaviors (*6*). The appearance of charge ordering (CO) or a Mott transition accompanied with dimeric distortion in a ¼-filled or a ¾-filled (¼-filled in terms of holes) network of A molecules with a one-dimensional (1D) or 2D structure plays a key role as the basis for these exotic natures (*1*, *2*). Recent theoretical studies have revealed that the critical balance among physical parameters, such as bandwidth (W), onsite Coulomb interaction (U), and nearest-neighbor Coulomb interaction (V), leads to the appearance of such novel ground states (*7*–*10*).

These previous studies and a report on the highly efficient photocarrier generation in one of the A_2B salts $(DCNQI)_2Cu$ (*11*) have stimulated research on the photoinduced phase transition (PIPT) in A_2B salts. In a crystal that shows multi-instability of its free energy due to critical balance among intrinsic cooperative interactions, the macroscopic phase transition accompanied with large changes in electronic, magnetic, and lattice structures may be triggered by weak photoexcitation (*12*, *13*), because even a low density of photoexcited species can affect and switch the cooperative interaction (*12*–*14*). From the viewpoint of the highly efficient and nonlinear amplification of the response to the weak photoexcitation via a cooperative channel in a condensed system, this exotic photo effect called PIPT is analogous to the "domino effect" on the molecular scale.

Here, we report that a quasi-1D, ¼-filled (in terms of holes) A_2B salt $(EDO\text{-}TTF)_2PF_6$ shows highly sensitive and ultrafast PIPT from an insulator (I) phase accompanied with a CO to a metal (M) phase up to about room temperature (~265 K). [EDO-TTF

[1]Department of Materials Science, Tokyo Institute of Technology, 2-12-1 Oh-okayama, Meguro-ku, Tokyo 152-8551, Japan. [2]Groupe Matière Condensée et Matériaux, Centre National de la Recherche Scientifique, Unite Mixte de Recherche-6626, Université de Rennes 1, Rennes, France. [3]Kanagawa Academy of Science and Technology and Japan Science and Technology Agency (JST), Precursory Research for Embryonic Science and Technology (PRESTO), 3-2-1, Sakado, Takatsu-ku, Kawasaki 213-0012, Japan. [4]Department of Physics, Tokyo Institute of Technology, Japan. [5]Division of Chemistry, Kyoto University, Sakyo-ku, Kyoto 606-8502, Japan. [6]Research Center for Low Temperature and Materials Science, Kyoto University, Sakyo-ku, Kyoto 606-8502, Japan. [7]High Energy Accelerator Research Organization (KEK) and [8]JST, Exploratory Research for Advanced Technology (ERATO), 1-1 O-ho, Tsukuba 305-0801, Japan. [9]Graduate School of Science and Technology, Chiba University 1-33, Yayoi-cho, Inage-ku, Chiba 263-8522, Japan.

*To whom correspondence should be addressed. E-mail: skoshi@cms.titech.ac.jp

(ethylenedioxytetrathiafulvalene) acts as an electron donor (D).] The origin of this exotic effect has been assigned to the photoinduced cooperative and nonequilibrium melting of a CO, based on time-resolved spectroscopic measurements. A dynamic study has revealed that the coherent phonon generation via electron-lattice (E-L) interaction seems to be strongly coupled with the observed highly efficient, so-called gigantic, photoinduced metallization process completed within 1.5 ps. In addition, the speed of recovery from the photoinduced M to the original I phase can be widely controlled by changing the excitation intensity (1 ps to 100 μs).

Recently, a quasi-1D, ¼-filled A_2B salt $(EDO\text{-}TTF)_2PF_6$ has been developed to realize an organic metal with strong E-L interaction that results from molecular deformations on a subnanometer scale (*15*). As expected, this crystal shows an exotic M-I phase transition that arises from CO, accompanied by a large structural change based on molecular deformation of EDO-TTF and a doubling of unit cells at room temperature (T_c = 278 K) (Fig. 1) (*15*–*18*). This M-I transition in $(EDO\text{-}TTF)_2PF_6$ can be sensitively probed spectroscopically, as plotted in Fig. 2A. The reflection band observed around 1.3 eV in the low-temperature I phase has been assigned to CT excitation among EDO-TTF (D) molecules accompanied by CO, i.e., excitation from D^+D^+ to $D^{2+}D^0$, directly reflecting the appearance of CO (*17*, *18*).

We prepared a crystal of $(EDO\text{-}TTF)_2PF_6$ with a surface of 0.1 mm by 0.2 mm using a previously reported method (*15*). We excited the crystal by laser light with a pulse width of 0.12 ps, and the excitation photon energy (1.55 eV) was nearly resonant to this CT band. The reflection spectra 10 ps before (Δt = –10 ps) and 3 ps after (Δt = 3 ps) the photoexcitation (Fig. 2B) were observed at 180 K and 265 K, with a resolution time of 0.25 ps. A similarly large and fast reflectivity change triggered by photoexcitation was confirmed in a wide temperature range below 265 K, and this change disappeared above T_c. The obtained spectral changes indicate that the intensity of the CT (D^+D^+ to $D^{2+}D^0$) band dramatically decreased and, in contrast, a rather weak and broad band, which seems to be characteristic of the M phase, appeared just after photoexcitation. Thus, CO melting, accompanied by I-M phase conversion, occurs within 3 ps after excitation by 0.12 ps light pulse. Movie S1 shows that the photoinduced modulation in reflectivity is large enough to be directly observed with an ordinary charge-coupled device camera after excitation with a white probe light 0.2 ps in width.

Compared with the reflectivity spectra of I and M phases under conditions of thermal equilibrium, the estimated photoinduced I-M conversion efficiency based on the reflectiv-

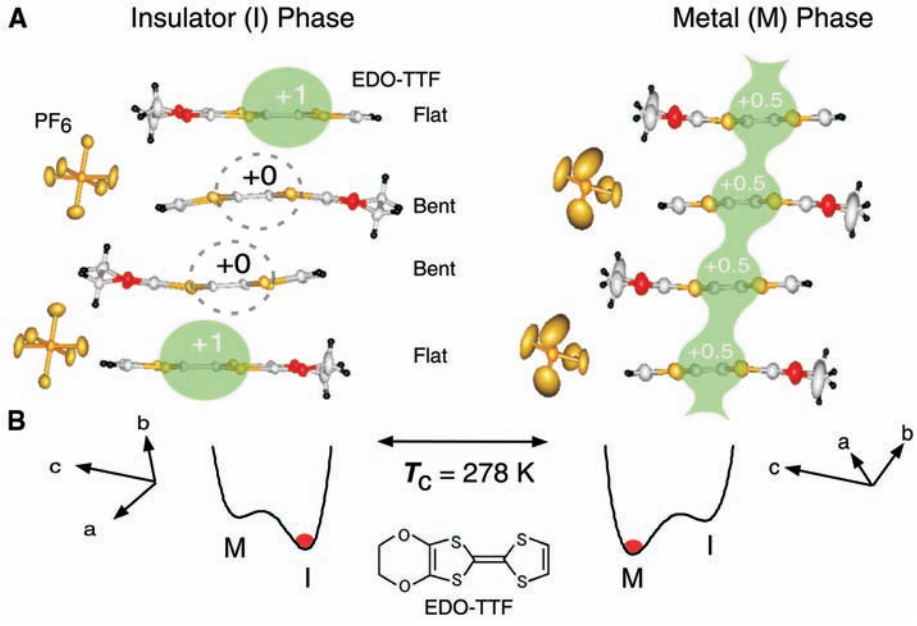

Fig. 1. (**A**) Schematic views of the lattice and electronic structural changes accompanying the M-I phase transition in $(EDO\text{-}TTF)_2PF_6$. A side view of an EDO-TTF molecule is shown. The unit cell includes two and four EDO-TTF molecules in M and I phases, respectively (*15*). In the I phase, holes are localized on EDO-TTF molecules with a flat structure due to CO, and quasi-neutral molecules show a bent structure. In the M phase, charges (holes) are delocalized and PF_6 (acceptor) molecules exhibit disorder (*15*–*18*). (**B**) Schematics for free-energy change accompanying M-I transition and the structure of the EDO-TTF molecule.

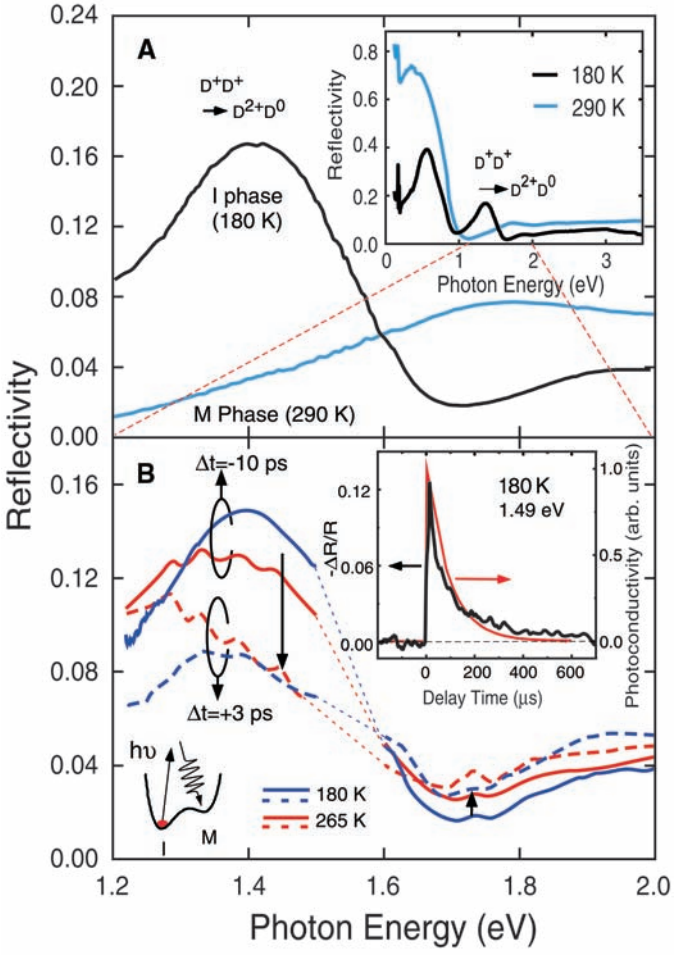

Fig. 2. (**A**) Reflectivity spectra for the M (blue line) and I (black line) phases observed at 290 and 180 K, respectively. (Inset) Reflectivity spectra in the wide photon energy region for the M (blue line) and I (black line) phases, respectively. (**B**) Reflectivity spectra observed at 10 ps before (Δt = –10 ps, solid lines) and 3 ps after (Δt = +3 ps, dashed lines) photoexcitation at the sample temperatures of 180 K (blue lines) and 265 K (red lines). The excitation density was 6×10^{18} cm^{-3} (*19*). The photoreflectivity spectra in the region between 1.5 and 1.6 eV could not be observed because of the strong scattering of the pump laser light. (Inset) Time profiles for $\Delta R/R$ at 1.49 eV (black line) and photoconductivity (red line) in the μs-ms region observed at 180 K.

ity change at Δt = 3 ps reached about 50% with an excitation intensity of 6 × 10^{18} photons cm^{-3}, corresponding to a single excitation photon for every 500 donor molecules (*19*). Such highly efficient conversion indicates a strong cooperative effect in this crystal, as expected from strong E-L coupling.

The inset in Fig. 2B shows the photoinduced reflectivity change ($\Delta R/R$) probed with 1.49 eV light and the photoconductivity at 180 K in the microsecond region with an excitation density of 6 × 10^{18} cm^{-3}. Both signals relaxed back to the original value within 300 to 400 μs. Thus, we could use light excitation with a 1 kHz repetition rate for a pump-probe experiment. The electric conductivity was largely enhanced (more than five orders of magnitude) just after photoexcitation within the resolution time (1 μs), which was consistent with the idea that the observed photoinduced effect arises from the I-M phase conversion.

A time profile of the spectral changes was observed at 1.38 and 1.72 eV with an excitation density of 6 × 10^{18} cm^{-3} (Fig. 3A). For Δt > 1.5 ps, the $\Delta R/R$ value remained constant, and the spectral shape was consistent with the I-M transition as a result of CO melting; thus, it can safely be concluded that the phase conversion process was completed within 1.5 ps for a wide temperature region. Such an ultrafast photoconversion process cannot be explained simply by the light-induced heating effect. In addition, as indicated by triangles in Fig. 3A, a vibrational structure with a large magnitude was observed. The period of this vibration, estimated from the interval between the first and second peaks [about 0.5 ps (70 cm^{-1}) at 180 K] has little dependence on the probe photon energy. Thus, this effect cannot be simply explained by strain-wave propagation induced by light excitation coupling with an acoustic mode as discussed previously (*20*–*22*).

As shown in the inset of Fig. 3A, several Raman modes in the low-energy region were observed for the I-phase crystal. The 84 cm^{-1} band observed at 180 K (red) softened as the sample temperature was increased (Fig. 3B, inset, red circles) (*23*). The same behavior has been observed in the temperature dependence of the vibration interval estimated from the time profiles of $\Delta R/R$ at various temperatures (Fig. 3B). The results are summarized and indicated in the inset of Fig. 3B by black squares. In addition, this vibrational mode was also Raman active in M phases (*23*). Based on these data, it is reasonable to attribute observed dynamic vibration in the time domain to the coherent phonon-like vibration that corresponds to this Raman-active optical mode, which exists even in the photoproduced M phase.

The present result indicates that the E-L interaction via the optical phonon mode plays important roles in driving the highly sensitive metallization process and stabilizing the photoinjected M domain. The vibrational mode calculation for a single EDO molecule in ionic and neutral states suggests the existence of several modes around a frequency region of 100 cm^{-1}, which can be attributed to a bending motion of the molecular plane (*23*). This result supports the idea that the observed coherent vibration in the $\Delta R/R$ time profile is due to strong coupling between CO and distortion of the molecular plane, which plays an essential role in thermally induced I-M transition in (EDO-

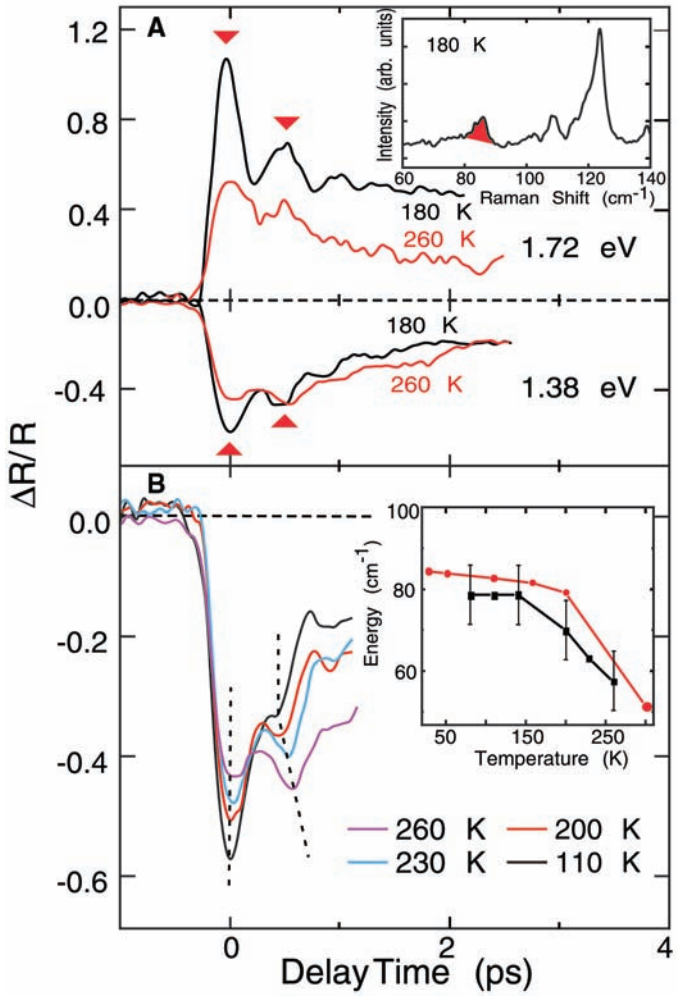

Fig. 3. (**A**) Probe photon energy dependence of the time profile for the $\Delta R/R$ observed at 180 K (black lines) and 260 K (red lines). The probe photon energy was 1.72 and 1.38 eV for the upper and lower panels, respectively. Triangles indicate the peak positions due to the vibratile structure observed at 180 K. (Inset) Raman spectrum in the low-energy region for the I phase observed at 180 K. Temperature dependence of the Raman shift energy for the red-colored mode is plotted in the inset of (**B**). (**B**) Temperature dependence of the time profile for the $\Delta R/R$ observed at 1.38 eV. (Inset) Temperature dependence of the Raman shift (red circles) for the red-colored mode in the inset of (**A**) and that for the vibratile frequency estimated from the time profile of $\Delta R/R$ (black squares). Error bars (mean ± SE) show the observed data fluctuations changing the sample crystal. The red and black lines serve as an eye guide.

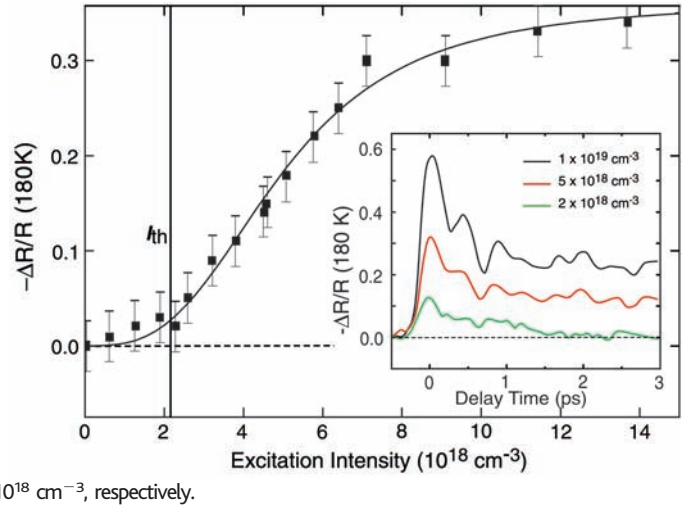

Fig. 4. Excitation intensity dependencies of $\Delta R/R$ observed 3 ps after excitation at 180 K. The black line is an eye guide, and I_{th} indicates the threshold photon density. The fluctuations in $\Delta R/R$ values due to the change of sample crystals even under the same excitation condition are indicated by error bars (mean ± SE) (**Inset**) Time profile of $\Delta R/R$ for various excitation photon densities observed at 180 K. The black, red, and green lines correspond to 1 × 10^{19}, 5 × 10^{18}, and 2 × 10^{18} cm^{-3}, respectively.

$TTF)_2PF_6$ (Fig. 1A). Of course, a further study for mode assignment is necessary to analyze the relation between molecular plane deformation and simple dimer distortion among unit cells, both of which play an important role to drive I-M transition.

One attractive aspect of PIPT is that the photoconversion efficiency shows a nonlinear dependence on the excitation intensity that reflects the role of cooperative interaction (*12*, *13*). In $(EDO\text{-}TTF)_2PF_6$, the photoreflectivity change probed with a 1.38 eV monitor light at 3 ps after photoexcitation showed a threshold-like behavior, with a critical absorbed photon density (I_{th}) of 2×10^{18} cm^{-3} (one photon for every 1500 EDO-TTF molecules) (*19*) (Fig. 4). The estimated heating temperature for the present experimental condition based on the thermodynamic data are only 0.1 K even for a 1×10^{19} cm^{-3} excitation intensity (*24*). Such a highly efficient and nonlinear conversion process is the result of internal cooperative interactions that are similar to other PIPT phenomena (*12*). In addition, the lifetime of the photoinduced M phase strongly depends on the excitation intensity (Fig. 4). This result supports a mechanism in which cooperative interactions occur even in the relaxation process of the photoinduced M phase. In the case of a 2×10^{18} cm^{-3} excitation condition, the $\Delta R/R$ signal disappeared within ~1.5 ps, which appears to facilitate a quick recovery time for applications in a phase-switching device.

To realize a molecular phase-switching device controllable by light with 1 ps (i.e., THz) response time, it is important to develop a material that shows highly sensitive and ultrafast PIPT phenomena at room temperature. One possible way to solve this problem is to use a phase transition due to the cooperation of spin, charge, and orbit degrees of freedom inherent in strongly correlated electrons (*25*–*29*). From our point of view, another way is to use an E-L coupled mechanism mediated by a coherent phonon process with large amplitude (*30*), a possibility discussed in pioneer works of ultrafast photo effect in VO_2 and a neutral-ionic transition system (*20*, *22*, *31*, *32*). In the case of an ordinal photoinduced domino effect, the speed of the domain growth process from photoinjected localized species to meso- or macroscopic regions accompanied by structural changes will be limited by an incoherent phonon process (*13*, *14*). In contrast, if the electronic lattice-coupled change is mediated by an optical phonon mode with k~0 via an E-L interacting channel, the phase change in the meso-size domain mediated by coherent phonons can be induced at once, immediately after photoexcitation.

The present results with $(EDO\text{-}TTF)_2PF_6$ show that this mechanism, the so-called "photo-domino on phonon coherence," seems to be useful for achieving this purpose, even at about room temperature. X-ray structural analysis and soft x-ray emission spectroscopy with femtosecond resolution, in addition to theoretical study, will be needed for clarifying the real mechanism of the observed gigantic photoinduced metallization and also will be important for molecular device–oriented research (*30*, *31*, *33*).

References and Notes

1. D. Jerome, H. J. Schulz, *Adv. Phys.* **51**, 293 (2002).
2. T. Ishiguro, K. Yamaji, G. Saito, Eds., *Organic Superconductors* (Springer-Verlag, Berlin-Heidelberg, ed. 2, 1998).
3. K. Bechgaard, C. S. Jacobsen, K. Mortensen, H. J. Pedersen, N. Thorup, *Solid State Commun.* **33**, 1119 (1980).
4. Y. Shimizu, K. Miyagawa, K. Kanoda, M. Maesato, G. Saito, *Phys. Rev. Lett.* **91**, 107001 (2003).
5. P. Monceau, F. Ya. Nad, S. Brazovskii, *Phys. Rev. Lett.* **86**, 4080 (2001).
6. H. Matsui *et al.*, *J. Phys. Soc. Jpn.* **70**, 2501 (2001).
7. J. E. Hirsch, D. J. Scalapino, *Phys. Rev. Lett.* **50**, 1168 (1983).
8. K. Penc, F. Mila, *Phys. Rev. B* **49**, 9670 (1994).
9. H. Seo, H. Fukuyama, *J. Phys. Soc. Jpn.* **66**, 1249 (1997).
10. D. Schmeltzer, A. Bishop, *Phys. Rev. B* **59**, 4541 (1999).
11. F. O. Karutz, J. U. von Schutz, H. Wachtel, H. C. Wolf, *Phys. Rev. Lett.* **81**, 140 (1998).
12. S. Koshihara, in *Optical Properties of Low-Dimensional Materials*, T. Ogawa, Y. Kanemitsu, Eds. (World Scientific, Singapore, 1998), vol. 2, chap. 3.
13. K. Nasu, Ed., *Photoinduced Phase Transition* (World Scientific, Singapore, 2004).
14. K. Koshino, T. Ogawa, *J. Phys. Soc. Jpn.* **67**, 2174 (1998).
15. A. Ota, H. Yamochi, G. Saito, *J. Mater. Chem.* **12**, 2600 (2002).
16. S. Aoyagi *et al.*, *Angew. Chem.* **43**, 3670 (2004).
17. O. Drozdova, K. Yakushi, A. Ota, H. Yamochi, G. Saito, *Synth. Met.* **133-134**, 277 (2003).
18. O. Drozdova *et al.*, *Phys. Rev. B* **70**, 075107 (2004).
19. Penetration depth at 1.55 eV excitation photon energy was estimated to be approximately 1 μm from the reflection spectrum using the Kramers-Kronig transformation method. The excitation light was assumed to be homogeneously absorbed in the surface region of the crystal with the thickness of 1 μm. As a result, the absorbed photon density used for the observation of photo effect shown in Fig. 2B was estimated to be 6×10^{18} photons/cm^3, corresponding to the excitation intensity of 6.4×10^{14} photons/cm^2. This photon density is approximately equal to a single excitation photon for every 500 donor molecules, based on the unit cell volume of 1170 $Å^3$ at 200 K and including four EDO-TTF molecules.
20. S. Iwai *et al.*, *Phys. Rev. Lett.* **88**, 057402 (2002).
21. T. Ogasawara *et al.*, *Phys. Rev. B* **68**, 180407 (2003).
22. K. Tanimura, I. Akimoto, *J. Lumin.* **94-95**, 483 (2001).
23. The frequency of the Raman mode was determined including the temperature dependence of the Bose factor. A detailed discussion including mode assignment is now in preparation for publication.
24. K. Saito, S. Ikeuchi, A. Ota, H. Yamochi, G. Saito, *Chem. Phys. Lett.*, in press.
25. G. Yu *et al.*, *Phys. Rev. B* **45**, 4964 (1992).
26. M. Fiebig, K. Miyano, Y. Tomioka, Y. Tokura, *Science* **280**, 1925 (1998).
27. T. Ogasawara, K. Tobe, T. Kimura, H. Okamoto, Y. Tokura, *J. Phys. Soc. Jpn.* **71**, 2380 (2002).
28. S. Iwai *et al.*, *Phys. Rev. Lett.* **91**, 057401 (2003).
29. S. Tomimoto, S. Miyasaka, T. Ogasawara, H. Okamoto, Y. Tokura, *Phys. Rev. B* **68**, 035106 (2003).
30. K. Sokolowski-Tintan *et al.*, *Nature* **422**, 287 (2003).
31. A. Cavalleri *et al.*, *Phys. Rev. Lett.* **87**, 237401 (2001).
32. K. Yonemitsu, *J. Phys. Soc. Jpn.* **73**, 2887 (2004).
33. A. Rousse, C. Rischel, J.-C. Gauthier, *Rev. Mod. Phys.* **73**, 17 (2001).

34. The authors are indebted to K. Yakushi and O. Drozdova of the Institute for Molecular Science for their participation in helpful discussions. This work was partially supported by grants-in-aid for scientific research and the 21st Century Center of Excellence programs from the Ministry of Education, Culture, Sports, Science, and Technology, Japan.

Supporting Online Material

www.sciencemag.org/cgi/content/full/307/5706/86/DC1
Movie S1

9 September 2004; accepted 23 November 2004
10.1126/science.1105067

Atom Collision–Induced Resistivity of Carbon Nanotubes

Hugo E. Romero,[1] Kim Bolton,[3] Arne Rosén,[3] Peter C. Eklund[1,2]*

We report the observation of unusually strong and systematic changes in the electron transport in metallic single-walled carbon nanotubes that are undergoing collisions with inert gas atoms or small molecules. At fixed gas temperature and pressure, changes in the resistance and thermopower of thin films are observed that scale as roughly $M^{1/3}$, where M is the mass of the colliding gas species (He, Ar, Ne, Kr, Xe, CH_4, and N_2). Results of molecular dynamics simulations are also presented that show that the maximum deformation of the tube wall upon collision and the total energy transfer between the colliding atom and the nanotube also exhibit a roughly $M^{1/3}$ dependence. It appears that the transient deformation (or dent) in the tube wall may provide a previously unknown scattering mechanism needed to explain the atom collision–induced changes in the electrical transport.

Single-walled carbon nanotubes (SWNTs) with diameters in the range from 1 to 2 nm exhibit quasi–one-dimensional (1D) electronic behavior, including strong van Hove singularities in the electronic density of states (*1*, *2*). Because all the carbon atoms reside at the tube surface, the chemical environment in contact with the nanotube can affect electron transport. The flow of a polar fluid over a nanotube film leads to an induced voltage along the direction of the flow (*3*), and the transconductance of a SWNT field effect transistor (FET)